

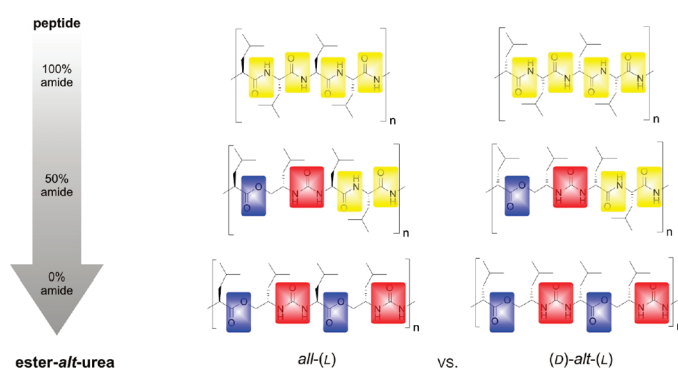
From Peptides to Their Alternating Ester-Urea Analogues: Synthesis and Influence of Hydrogen Bonding Motif and Stereochemistry on Aggregation

Sebastian Hartwig, Jutta Schwarz, and Stefan Hecht*

Department of Chemistry, Humboldt-Universität zu Berlin, Brook-Taylor-Strasse 2, 12489 Berlin, Germany

sh@chemie.hu-berlin.de

Received October 29, 2009



Peptide-mimicking scaffolds with an incorporated ester-urea motif, replacing two adjacent amide residues, were synthesized and their aggregation behavior was studied in dependence of hydrogen bonding sites as well as backbone stereochemistry. Two oligomer series containing either 50% or 100% ester-urea units and either *all*-(L) or (D)-*alt*-(L) backbone configuration were prepared via ester and amide couplings, using a divergent/convergent exponential growth strategy. Their aggregation behavior in organic solution was investigated by means of concentration-dependent NMR spectroscopy and compared to the parent peptide series. Interestingly, the naturally occurring peptide scaffold exhibits the largest tendency to associate in combination with the strongest difference in aggregation behavior between *all*-(L) and (D)-*alt*-(L) backbone stereochemistry. With increasing incorporation of the ester-urea motif the aggregation strength decreases and become much less dependent on the backbone configuration. The obtained structure–aggregation relationships reveal the importance of the commensurability and multivalency of hydrogen bonding sites as well as conformational restriction for peptide association and should hence aid the design of peptide mimics, such as β -sheet breakers or gelators.

Introduction

The generation and elucidation of peptide structures is crucial for both understanding biological processes and developing biologically active materials suitable for pharmaceutical and medical applications.¹ With this in mind, it becomes apparent that not only the development of new

peptides is an important field of research,² but also the integration of other functionalities into the polyamide backbone of a peptide is promising to gain detailed insight into structure–function relationships, subsequently leading to improved properties.³

One possibility of varying the backbone of a peptide is the replacement of amides with esters. For incorporation of an ester as an isostere into the sequence, an α -amino acid needs to be exchanged by an α -hydroxy acid. This replacement

(1) (a) Marx, V. *Chem. Eng. News* **2005**, 83, 17. (b) Gentilucci, L.; Tolomelli, A.; Squassabia, F. *Curr. Med. Chem.* **2006**, 13, 2449.

(2) (a) *Peptide-Based Drug Design: Methods and Protocols*; Otvos, L., Ed; Springer, Berlin, Germany, 2008; (b) Caliceti, P.; Veronese, F. M. *Adv. Drug Delivery Rev.* **2003**, 55, 1261. (c) *Trends and Future Perspectives in Peptide and Protein Drug Delivery*; Lee, V., Ed.; Taylor & Francis: New York, 1995.

(3) (a) *Advances in Amino Acid Mimetics and Peptidomimetics*; Abell, A. D., Ed.; JAI Press: New York, 1999; Vol. 2. (b) *Pseudo-Peptides in Drug Discovery*; Nielsen, P. E., Ed.; Wiley-VCH: Weinheim, Germany, 2004.

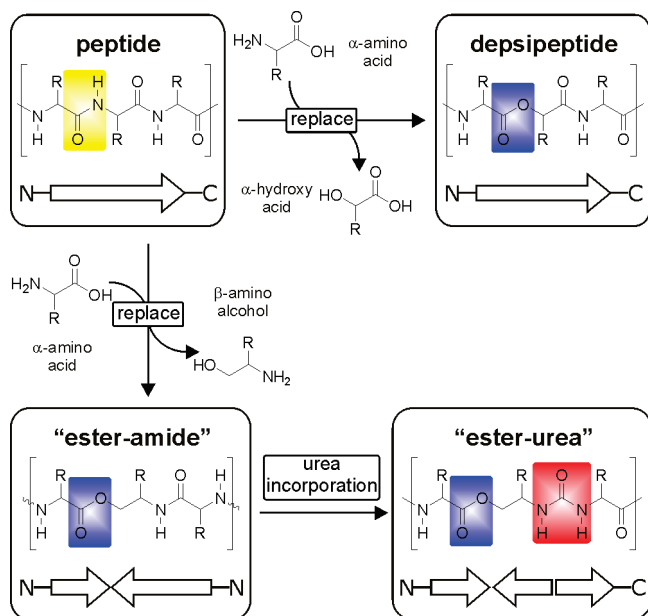


FIGURE 1. Peptide backbone modifications leading to depsipeptides, "ester-amides", and novel structural motifs, such as the investigated "ester-ureas".

maintains the direction of the peptide sequence (i.e., from *N*- to *C*-terminus) but eliminates one hydrogen bond donor site (see Figure 1 on top). This field of depsipeptides has been thoroughly investigated over the past decades,⁴ in particular with regard to folding behavior.

Another interesting possibility to exchange an amide by an ester is the replacement of an α-amino acid in the sequence by the corresponding amino alcohol (see Figure 1, bottom left). This exchange introduces an ester under elongation⁵ of the backbone by one atom and eliminates one hydrogen bond acceptor site. This amide-ester exchange goes in hand with a reversal of the main chain direction in the ester-amide backbone.

One option to maintain the direction of the peptide is the further incorporation of a urea moiety into the backbone,⁵ so that altogether two adjacent amino acids in the peptide are

replaced by an "ester-urea" moiety (see Figure 1, bottom right). This urea incorporation elongates⁶ the backbone by one further atom and adds one hydrogen bond acceptor. The ester-urea structure has the same main chain direction as the original peptide and also the same number of hydrogen bond donor and acceptor sites. The location and the direction of these hydrogen bond donors and acceptors in the backbone differ significantly from those in peptides. The incorporation of an ester interrupts the highly ordered hydrogen bonding pattern of the peptide backbone, whereas the urea unit is engaged in stronger hydrogen bonding interactions and hence may be able to compensate.^{7,8} This linkage variation results in a very interesting type of hydrogen bonding pattern and thereby in a potentially novel secondary (and higher) structure(s). Consequent replacement of every amide in the main chain affords an ester-*alt*-urea backbone, which constitutes an interesting and novel class of compounds with potentially advantageous properties, such as improved biodegradability and bioavailability. In addition to linkage chemistry the incorporation of (D)-configured amino acid building blocks presents another means to largely affect peptide secondary structures, e.g., in the alternating (D)-*alt*-(L) Gramicidin channels,^{9,10} thereby causing significantly different pharmacological characteristics.

This simple structural gedankenexperiment encouraged us to prepare and investigate oligomers with varying degree of ester-urea incorporation and different stereochemistry, i.e. *all*-(L) and (L)-*alt*-(D).¹¹ Here, we present the synthesis of these two new peptide mimicking backbones and report some initial investigations of the association behavior of their short oligomers.

Results and Discussion

General Design Considerations. To investigate the influence of the connectivity (isostere incorporation) and stereochemistry, three different series ranging from peptides to completely alternating ester-urea pseudopeptides each composed of both

(6) Elongation refers to the side chain repetition, i.e., the number of atoms in between neighboring monomer repeat units.

(7) Ureas have been used to facilitate aggregation and subsequent crystallization or gelation: (a) Desiraju, G. R., *Crystal Engineering: The Design of Organic Solids*; Elsevier: Amsterdam, The Netherlands, 1989; (b) Jadzyn, J.; Stockhausen, M.; Zywucki, B. *J. Phys. Chem.* **1987**, *91*, 754. (c) Chang, Y.-L.; West, M.-A.; Fowler, F. W.; Lauher, J. W. *J. Am. Chem. Soc.* **1993**, *115*, 5991. (d) van Esch, J. H.; Kellogg, R. M.; Feringa, B. L. *Tetrahedron Lett.* **1997**, *38*, 281. (e) van Esch, J. H.; Schoonbeek, F.; de Loos, M.; Kooijman, H.; Spek, A. L.; Kellogg, R. M.; Feringa, B. L. *Chem.—Eur. J.* **1999**, *5*, 937. (f) van Esch, J. H.; Feringa, B. L. *Angew. Chem., Int. Ed.* **2000**, *39*, 2263. (g) Schoonbeek, F. S.; van Esch, J. H.; Hulst, R.; Kellogg, R. M.; Feringa, B. L. *Chem.—Eur. J.* **2000**, *6*, 2633. (h) de Loos, M.; Ligtenbarg, A. G. J.; van Esch, J. H.; Kooijman, H.; Spek, A. L.; Hage, R.; Kellogg, R. M.; Feringa, B. L. *Eur. J. Org. Chem.* **2000**, 3675. For a theoretical treatment of urea aggregation, see: (i) Stumpe, M. C.; Grubmüller, H. *J. Phys. Chem. B* **2002**, *111*, 6220.

(8) For reviews on small molecule gelators based on amides and ureas, see: (a) Estroff, L. A.; Hamilton, A. D. *Chem. Rev.* **2004**, *104*, 1201. (b) Fages, F.; Vögtle, F.; Zinic, M. *Top. Curr. Chem.* **2005**, *256*, 77.

(9) (a) Wallace, B. A.; Ravikumar, K. *Science* **1988**, *241*, 182. (b) Langs, D. A. *Science* **1988**, *241*, 188. (c) Hladky, S. B.; Haydon, D. A. *Nature* **1970**, *523*, 451.

(10) For artificial (D)-*alt*-(L) peptides, see for example: (a) Benedetti, E.; Di Blasio, B.; Pedone, C.; Lorenzi, G. P.; Tomasic, L.; Gramlich, V. *Nature* **1979**, *282*, 630. (b) Lorenzi, G. P.; Tomasic, L. *Makromol. Chem.* **1988**, *189*, 207. (c) Di Blasio, B.; Benedetti, E.; Pavone, V.; Pedone, C.; Spiniello, O.; Lorenzi, G. P. *Biopolymers* **1989**, *28*, 193.

(11) For related recent investigations, see: (a) Hartwig, S.; Hecht, S. *Macromolecules*. DOI: 10.1021/ma902018w. Published Online: Oct 30, 2009. (b) Hartwig, S.; Nguyen, M. M.; Hecht, S. *Polym. Chem.* DOI:10.1039/B9PY00217K. Published Online.

(4) For selected examples, see: (a) Shemyakin, M. M. *Angew. Chem.* **1960**, *72*, 342. (b) Schwyzer, R.; Carrion, J. P. *Helv. Chim. Acta* **1960**, *43*, 2101. (c) Schulz, H. *Chem. Ber.* **1966**, *99*, 3425. (d) Shemyakin, M. M.; Shchukina, L. A.; Vinogradova, E. I.; Ravdel, G. A.; Ovchinnikov, Yu. A. *Experientia* **1966**, *22*, 535. (e) Ingwall, R. T.; Goodman, M. *Macromolecules* **1974**, *7*, 598. (f) Becktel, W.; Wouters, G.; Simmons, D. M.; Goodman, M. *Macromolecules* **1985**, *18*, 630. (g) Goodman, M. *Biopolymers* **1985**, *24*, 137. (h) Gallo, E. A.; Gellman, S. H. *J. Am. Chem. Soc.* **1993**, *115*, 9774. (i) Katakai, R.; Kobayashi, K.; Yonezawa, N.; Yoshida, M. *Biopolymers* **1996**, *38*, 285. (j) Karle, I. L.; Das, C.; Balaran, P. *Biopolymers* **2001**, *59*, 276. (k) Jude, A. R.; Providence, L. L.; Schmutzer, S. E.; Shobana, S.; Greathouse, D. V.; Andersen, O. S.; Koeppel, R. E. *Biochemistry* **2001**, *40*, 1460. (l) Oku, H.; Yamada, K.; Katakai, R. *Biopolymers* **2008**, *89*, 270.

(5) For examples of urea incorporation into peptides, see: (a) Rink, H. *Tetrahedron Lett.* **1987**, *28*, 3787. (b) Burgess, K.; Linticum, D. S.; Shin, H. *Angew. Chem., Int. Ed.* **1995**, *34*, 907. (c) Kim, J. M.; Bi, Y.; Paikoff, S.; Schultz, P. G. *Tetrahedron Lett.* **1996**, *37*, 5305. (d) Burgess, K.; Ibarzo, J.; Linticum, D. S.; Russell, D. H.; Shin, H.; Shitang-Koon, A.; Totani, R.; Zhang, A. J. *J. Am. Chem. Soc.* **1997**, *119*, 1556. (e) Boeijen, A.; Liskamp, R. M. J. *Eur. J. Org. Chem.* **1999**, 2127. (f) Guichard, G.; Semetey, V.; Rodriguez, M.; Briand, J.-P. *Tetrahedron Lett.* **2000**, *41*, 1553. (g) Semetey, V.; Rognan, D.; Hemmerlin, C.; Graff, R.; Briand, J.-P.; Marraud, M.; Guichard, G. *Angew. Chem., Int. Ed.* **2002**, *85*, 1893. (h) Hemmerlin, C.; Marraud, M.; Rognan, D.; Graff, R.; Semetey, V.; Briand, J.-P.; Guichard, G. *Helv. Chim. Acta* **2002**, *85*, 3692. (i) Sureshbabu, V. V.; Patil, B. S.; Venkataramanarao, R. J. *Org. Chem.* **2006**, *71*, 7697.

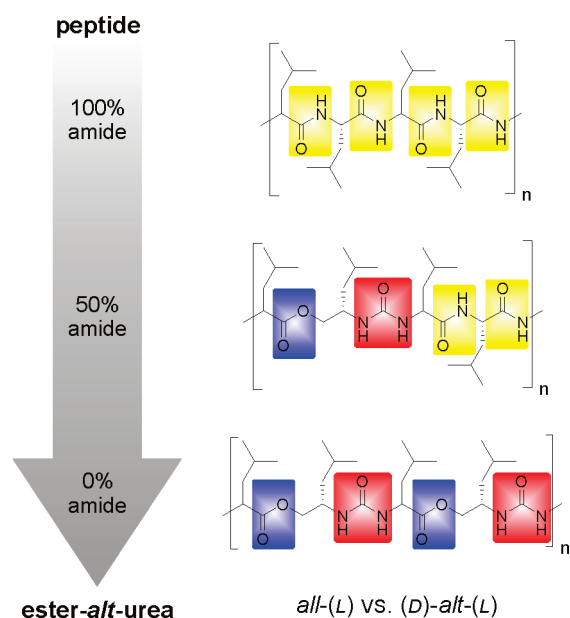


FIGURE 2. Two adjacent amide bonds in the peptide backbone (highlighted in yellow) are successively replaced by an ester-*alt*-urea moiety (ester highlighted in blue, urea highlighted in red).

all-(L)- as well as (D)-*alt*-(L)-configured amino acid building blocks (Figure 2) were targeted.

Oligo-(L)- and oligo-(D)-*alt*-(L)-peptides having an amide content of 100% (Figure 2, top) serve as reference compounds. As a first structural variation, half of the amide bonds of the peptide backbone can be replaced by an ester-*alt*-urea moiety (Figure 2, middle). Complete replacement of the amide bonds leads to alternating ester-urea pseudopeptides (Figure 2, bottom). Note that incorporation of the ester-urea motif allows for variation of the stereochemistry, leading to *all*-(L)- as well as (D)-*alt*-(L)-structures in the latter two cases. Interestingly, such trivial structural variation leads to two new backbone primary structures, which, to the best of our knowledge, have not been reported thus far. To restrict structural variations to connectivity and stereochemistry only, strands based solely on leucine and leucine were investigated, as leucine carries no functionality in the side chain, therefore facilitating synthesis. Furthermore, we limit the discussion to the tetramer series ($n = 1$).

Synthesis. Synthesis of the Key Building Block. The synthesis of the different targeted series of compounds with variable stereochemistry (Figure 2) requires a straightforward strategy based on coupling of common fragments. The native peptides are readily accessible via a divergent/convergent synthesis. The 50% and 0% amide containing pseudopeptides can be derived from a common key building block, largely minimizing the synthetic effort (Figure 3).

This key building block can readily be synthesized by reaction of (L)-Leu-Bn and (D)-Leu-Bn, respectively, with 1,1'-carbonyldiimidazole (CDI) and subsequent coupling with (L)-leucine, to give both the *all*-(L)- as well as the (L)-*alt*-(D)-diastereomers **3a** and **3b** in good yields (Scheme 1).¹¹ The benzyl ester protecting group can quantitatively be cleaved by hydrogenolysis with use of Pd/C under a hydrogen atmosphere. Alternative cleavage conditions involving saponification led to undesired, quantitative cyclization to the corresponding hydantoin during the acidic aqueous workup

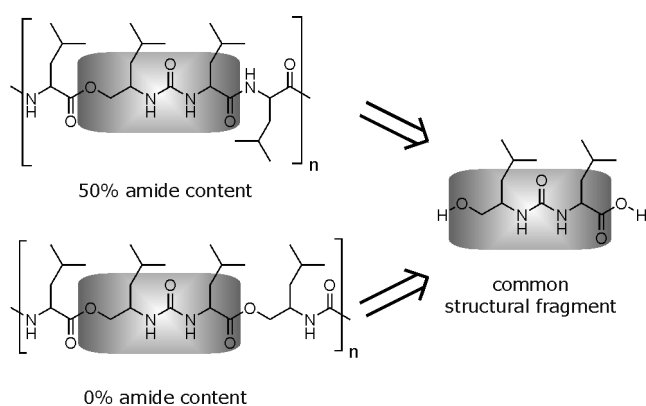
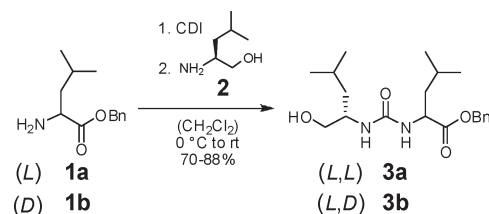


FIGURE 3. Key building block for pseudopeptide synthesis.

SCHEME 1. Synthesis of the Key Building Blocks **3a/3b**



procedure, as experienced in the attempted cleavage of the methyl ester protected leucine ureas.¹²

Synthesis of the Ester-*alt*-Urea Pseudopeptide Series. With the key building blocks **3a** and **3b** in hand, the ester-*alt*-urea tetramers can readily be synthesized via divergent/convergent synthesis. One requirement for divergent/convergent synthesis is the protection of both reactive chain ends with orthogonal protecting groups, in order to prevent undesired polymerization and to enable selective activation of each terminus. While a benzyl ester served to protect the carboxylic acid, the alcohol functionality was protected with the *tert*-butyldiphenylsilyl (TBDPS) group, allowing for orthogonal deprotection by hydrogenolysis and fluoride, respectively. The TBDPS-group showed superior hydrolytic stability as compared to both triisopropylsilyl (TIPS) as well as *tert*-butyldimethylsilyl (TBDMS).¹²

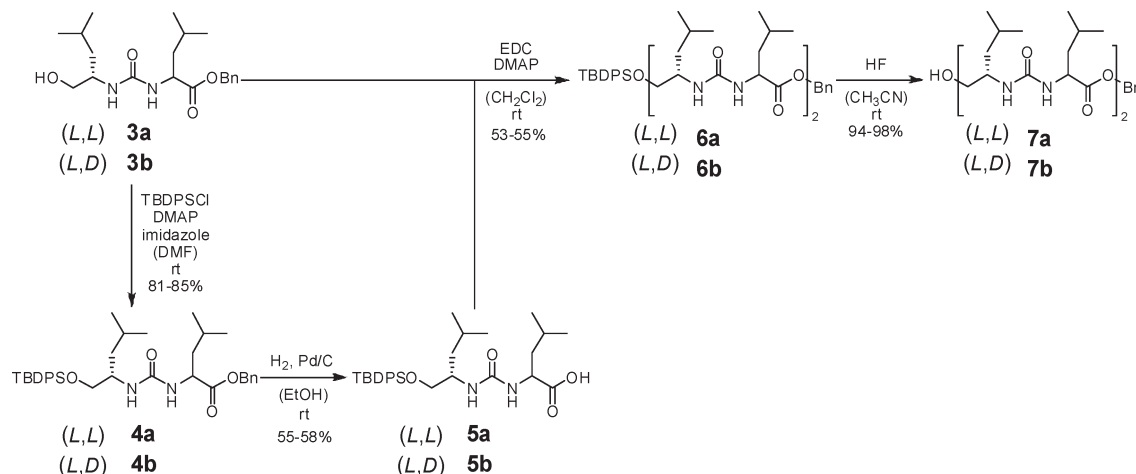
Starting from **3a/3b**, a TBDPS incorporation followed by hydrogenolysis led to **5a/5b**, which were then coupled to **3a/3b** to afford the fully protected tetramers **6a/6b** (Scheme 2). An esterification protocol, involving 1-(3-dimethylamino-propyl)-3-ethylcarbodiimide hydrochloride (EDC) as coupling reagent and 4-dimethylaminopyridine (DMAP) as the catalyst (*vide infra*),¹³ was employed. Finally, the TBDPS-protecting group was removed with HF in acetonitrile to yield the desired ureas **7a/7b** in high yields after column chromatography.

Synthesis of the 50% Amide Containing Pseudopeptide Series. The synthesis of the oligopseudopeptides with 50% amide content was initiated by the formation of an ester bond between key building blocks **3a/3b** and Boc-protected leucine (Scheme 3). Since first esterification attempts suffered from poor yields and difficult purifications, the reaction was screened extensively in order to elaborate the best

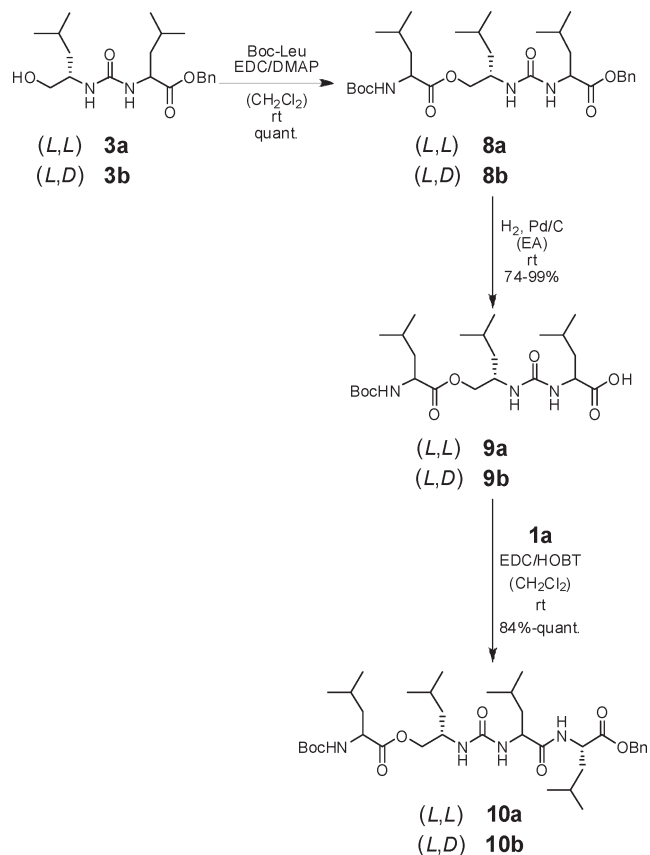
(12) See the Supporting Information.

(13) (a) Höfle, G.; Steglich, W.; Vorbrüggen, H. *Angew. Chem., Int. Ed. Engl.* **1978**, *17*, 569. (b) Scriven, E. F. V. *Chem. Soc. Rev.* **1983**, *12*, 129.

SCHEME 2. Synthesis of the *all*-(L)- and (L)-*alt*-(D)-Tetramers 7a/7b via a Divergent/Convergent Synthesis Approach, Starting from the Key Building Blocks 3a and 3b, Respectively



SCHEME 3. Synthesis of the 50% Amide Containing *all*-(L)- and the (D)-*alt*-(L)-Tetrapseudopeptides 10a and 10b, Respectively, Starting from the Key Building Blocks 3a and 3b



coupling conditions and workup procedures.¹² Summarizing the results from this screening, it is important to point out the role of the coupling catalysts for esterification. 1-Hydroxybenzotriazole (HOBT), which is one of the catalysts of choice for peptide bond formation because of its high reactivity and its low degree of peptide epimerization, was by far not the best coupling catalyst in our esterification reactions. It

turned out that DMAP¹³ and 4-dimethylaminopyridinium tosylate (DPTS)¹⁴ gave much better results, quite independently from the coupling reagent. Furthermore, the typically performed aqueous workup procedure was replaced by an alternative method involving stirring the crude reaction mixture over silica gel immediately followed by chromatography. On the basis of this optimized protocol, the reaction was performed on gram scales and afforded the resulting products **8a** and **8b** in quantitative yields and in high purity.

Subsequently, the trimers **8a** and **8b** were deprotected at their C-termini via hydrogenolysis to yield the desired products **9a** and **9b** in quantitative yields after purification via silica column chromatography. Subsequent coupling with C-protected leucine **1a** gave the *all*-(L)- and (L)-*alt*-(D)-ester-*alt*-urea-tetramers **10a** and **10b** in high yields and purities. In principle, the desired tetramers **10a/10b** could also be obtained by extending **3a/3b** at the C-terminus first and esterification of the alcohol in the last step; however, this “amide-first” route was not successful.³ Note that the orthogonally protected tetramers **10a** and **10b** enabled further growth of the pseudopeptides via a divergent/convergent synthesis approach up to the stages of octamers as well as hexadecamers.¹²

Synthesis of the Peptide Series. The reference (D)-*alt*-(L)- and *all*-(L)-leucine tetramers were synthesized via a divergent/convergent synthesis, involving the orthogonally Boc/Bn-ester protected dileucine building block, which is readily available by coupling either (L)- or (D)-*N*-Boc-protected leucine with (L)-*C*-Bn-protected leucine.¹² Note that solution synthesis instead of well-established solid phase supported peptide synthesis was used with the option to prepare the desired peptides on multigram scales.

All of the compounds synthesized constitute rather small leucine-based oligomers, differing in the stereochemistry of the backbone repeat units and their connecting motifs. Due to the replacement of amide bonds by ester-*alt*-urea moieties, a significant change in hydrogen bonding pattern and hence resulting structure formation was anticipated. Therefore, the eminent structural differences of these compounds were expected to largely affect their intermolecular interactions in solution, leading to a significantly altered aggregation behavior. Note that the present oligomers are of insufficient

(14) Moore, J. S.; Stupp, S. I. *Macromolecules* **1990**, *23*, 65.

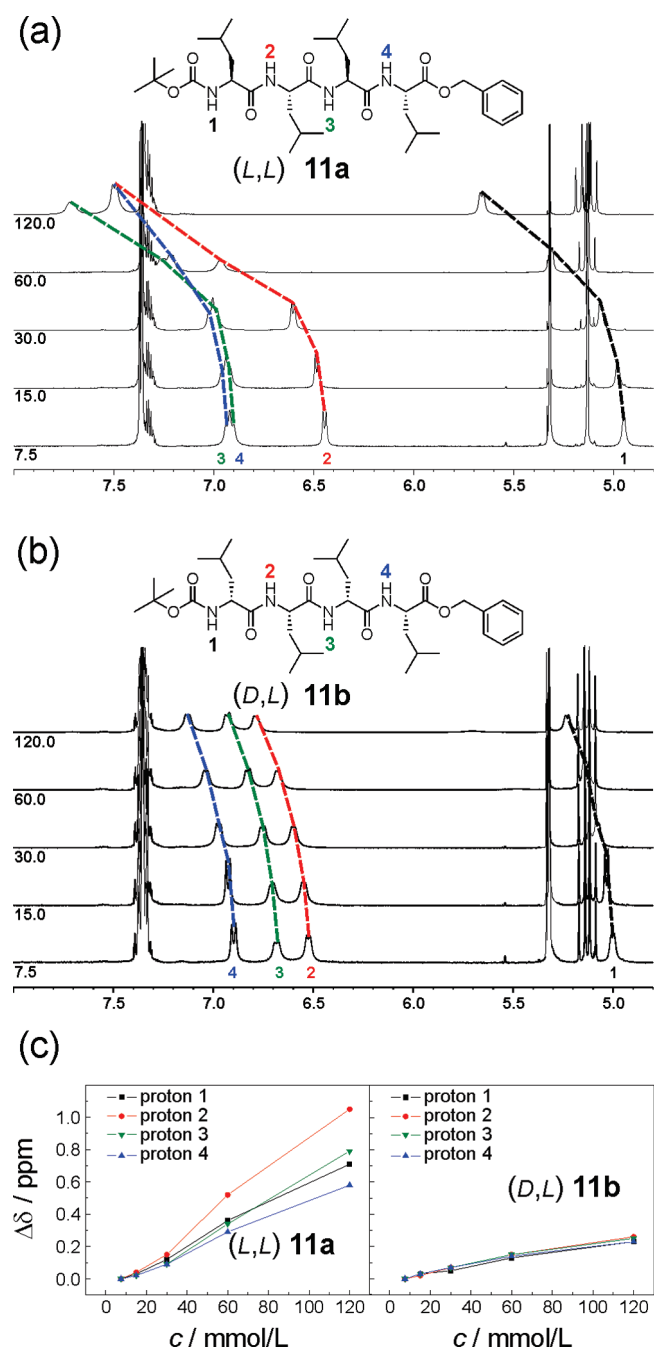


FIGURE 4. ¹H NMR spectra of (a) *all*-(L)-tetrapeptide **11a** and (b) (D)-*alt*-(L)-tetrapeptide **11b** at varying concentrations. (c) Proton chemical shift differences as a function of concentration for peptides **11a** and **11b**. All spectra were recorded in CD₂Cl₂ at 25 °C.

chain length to allow for intramolecular secondary structure formation, in particular folding into helical structures.

NMR Aggregation Studies. To investigate the aggregation of the various oligomers, NMR spectroscopy constitutes a versatile tool, since the protons involved in hydrogen bonding interactions are expected to display characteristic shifts

in their spectra upon changing the concentration.¹⁵ As a consequence of the limited length of the oligomers all proton signals are well separated and can be assigned by using COSY and NOESY measurements, carried out at concentrations below the aggregation threshold (7.5 mmol/L).¹⁶ Once every relevant proton in the spectrum was correctly attributed to the corresponding signal, aggregation could be monitored by the downfield shift of the amide or urea protons over a concentration range from 7.5 to 120 mmol/L,¹⁷ providing insight into both the overall aggregation tendency as well as the specific interacting regions of the molecules. Note that higher levels of hierarchical self-assembly, such as fiber formation typically resulting in gelation, occur at even higher concentrations and are not the subject of the presented study.

The choice of the solvent for these studies is crucial for several reasons. On the one hand, protons involved in the aggregation process, which is primarily mediated by hydrogen bonding, are all exchanging protons and thus protic solvents, such as water or alcohols, leading to fast proton exchange could not be used. On the other hand, the interaction of the compounds with the solvent should not disfavor aggregation and hence, hydrogen bond competitors, such as strongly solvating DMF or DMSO, had to be excluded. Furthermore, the solvent should be capable of dissolving all compounds even at higher concentrations, eliminating acetonitrile as well as all apolar solvents, such as hexane or toluene. Considering all these restrictions, CD₂Cl₂ was the solvent of choice¹⁸ for the aggregation studies, although excluding variable-temperature experiments well above 25 °C.

The concentration series of the peptides shows a markedly different behavior for the *all*-(L)-tetrapeptide **11a** as compared to the (D)-*alt*-(L)-tetrapeptide **11b** (Figure 4). Clearly, **11a** experiences much more pronounced downfield shifts as compared to **11b**, suggesting much stronger association. When looking at the individual shifts, **11b** displays very similar behavior for all four protons. In contrast, the inner amide protons labeled 2 and 3 (as well as the carbamate proton 1) of **11a** exhibit larger chemical shift differences than the outer amide proton 4, pointing to particular stabilization of the aggregate by formation of hydrogen bonds in the core. In the case of **11a**, the terminal benzylic protons display a characteristic splitting at high concentration, while in **11b** these benzylic protons are split even at low concentration and one may therefore speculate about local conformational restriction within **11a**, for example, by loop formation.

Contrasting the studies of the tetrapeptides, the concentration-dependent spectra of the partial ester-urea series, in general, show smaller shift differences (Figure 5). Again, more pronounced downfield shifts were observed for the *all*-(L)-tetramer **10a** as compared to the (D)-*alt*-(L)-analogue **10b**. Similar to the peptide case, the four protons in **10a** exhibit rather different shifts of their signals in comparison to **10b**. Notably, one of the urea protons (3) in **10a** experiences

(16) Below this concentration (7.5 mmol/L), ¹H NMR chemical shifts remained constant, indicating the absence of intermolecular interaction, i.e., hydrogen bonds, and hence exclude aggregation.

(17) Larger concentrations could hardly be realized as the solutions became rather viscous.

(18) Due to its potential decomposition liberating HCl, CDCl₃ was not used as an alternative solvent as the aggregation process should be pH-dependent.

(15) (a) Meraldy, J. P.; Hrubby, V. J. *J. Am. Chem. Soc.* **1976**, *98*, 6408. (b) Higashijima, T.; Tasumi, M.; Miyazawa, T.; Miyoshi, M. *Eur. J. Biochem.* **1978**, *89*, 543. (c) Iqbal, M.; Balam, P. *Biochemistry* **1981**, *20*, 7278. (d) Iqbal, M.; Balam, P. *Biopolymers* **1982**, *21*, 1427. (e) Raj, P. A.; Balam, P. *Biopolymers* **1985**, *24*, 1131.

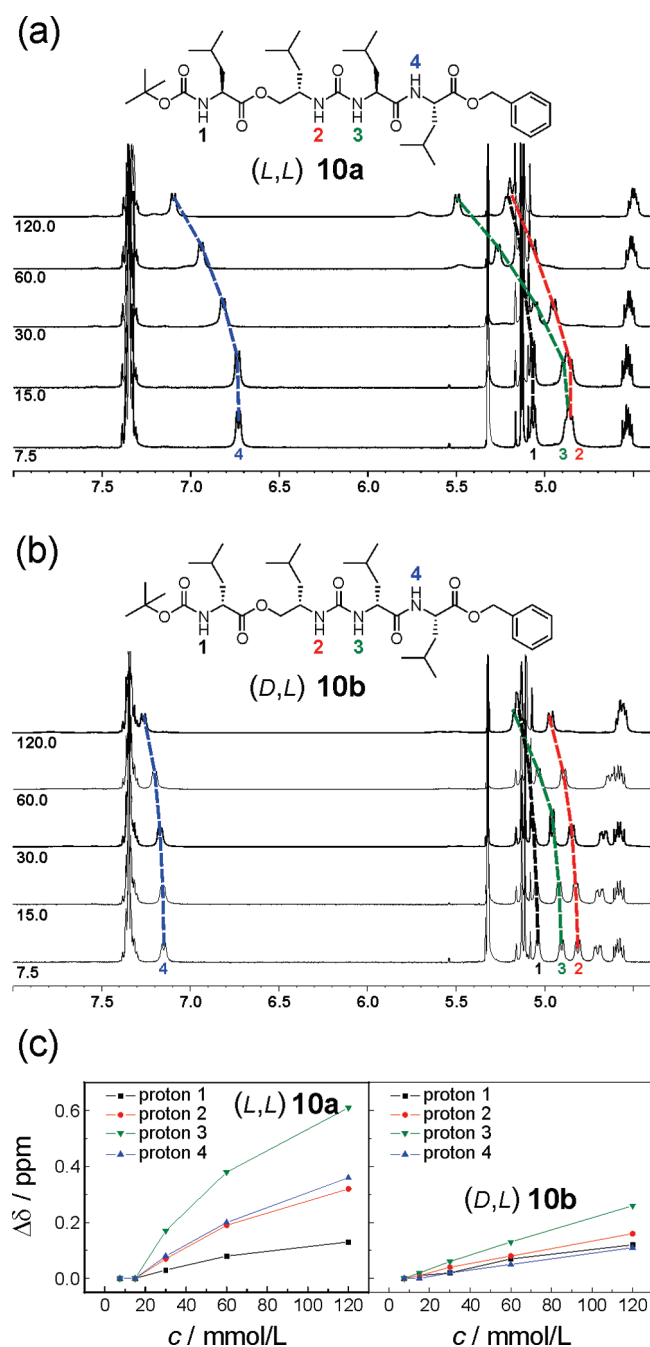


FIGURE 5. ¹H NMR spectra of (a) *all*-(L)-tetramer **10a** and (b) (D)-*alt*-(L)-tetramer **10b** at varying concentrations. (c) Proton chemical shift differences as a function of concentration for peptides **10a** and **10b**. All spectra were recorded in CD₂Cl₂ at 25 °C.

a much larger shift as compared to the other urea proton (2), suggesting that the urea moiety engages in a nonsymmetric hydrogen bond. The same is true for the urea protons in **10b**; however, the chemical shift differences are much smaller.

Last but not least, inspection of the concentration-dependent NMR spectra of the exclusive ester-urea series reveals that the shift differences are of the same magnitude for both the *all*-(L)-tetramer **7a** and the (D)-*alt*-(L)-tetramer **7b** (Figure 6). In both cases, the chemical shift differences are comparable to those of **10a**, suggesting a similar association strength. When analyzing the contributions of the individual

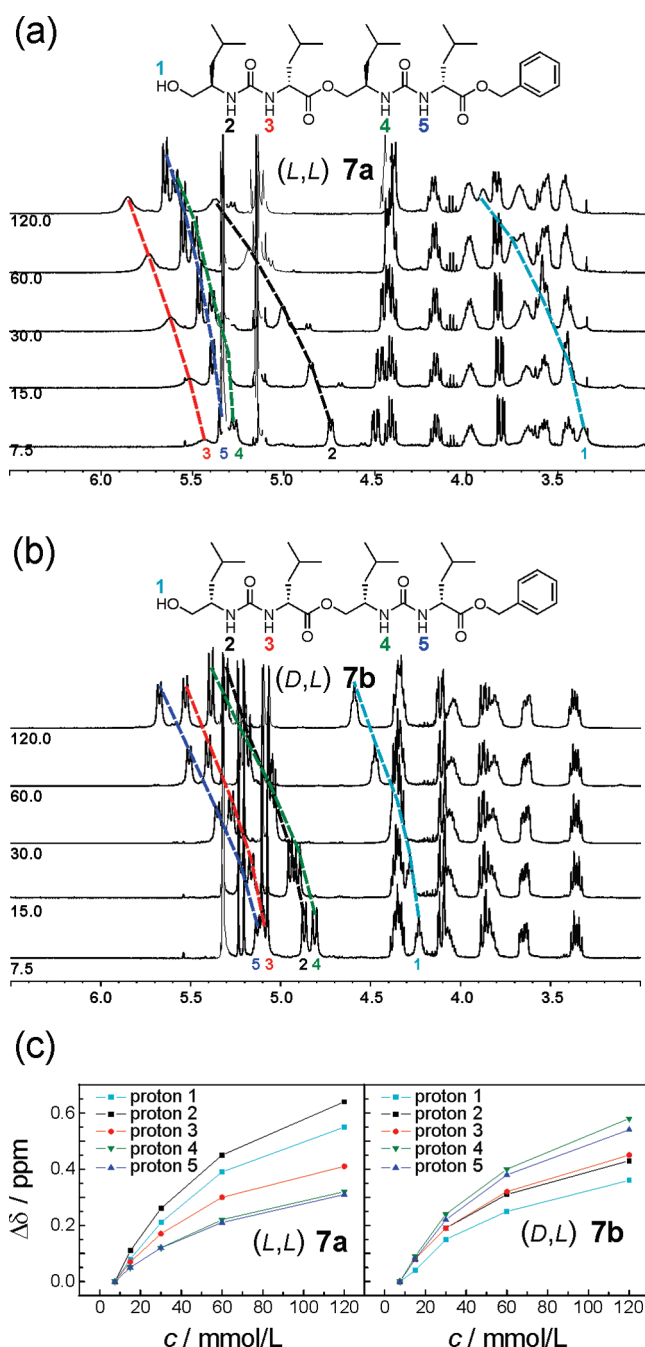


FIGURE 6. ¹H NMR spectra of (a) *all*-(L)-tetramer **7a** and (b) (D)-*alt*-(L)-tetramer **7b** at varying concentrations. (c) Proton chemical shift differences as a function of concentration for peptides **7a** and **7b**. All spectra were recorded in CD₂Cl₂ at 25 °C.

protons, both urea moieties in **7b** seem to be involved in rather symmetrical hydrogen bonding interactions, as the chemical shifts of protons 4 and 5 as well as 2 and 3 are nearly identical. In contrast, one of the urea moieties in **7a** shows rather distinct chemical shift differences (protons 2 and 3), while the other urea moiety is associated with equal chemical shift differences (protons 4 and 5). Hence, the urea units in **7a** seem to engage in both symmetrical as well as nonsymmetrical hydrogen bonding interactions.

The aggregation tendencies of the six investigated tetramers can be summarized as follows: The native, natural

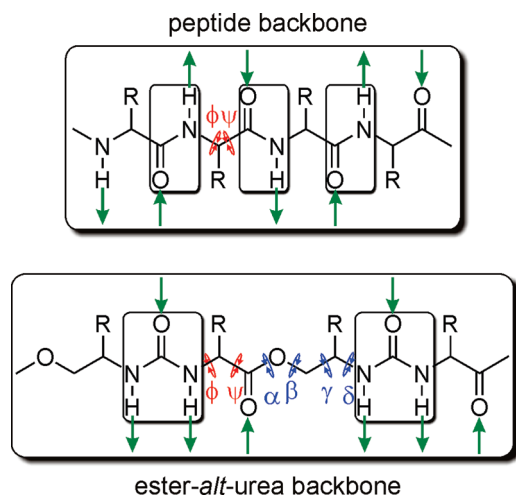


FIGURE 7. Comparison of peptide and ester-*alt*-urea backbones with regard to conformational freedom and hydrogen bonding pattern. Hydrogen bonding donor and acceptor sites are indicated with green arrows and show the commensurability in the case of the peptide only. In the peptide, rotational angles ϕ and ψ are displayed in red, while in the case of ester-*alt*-ureas additional rotational angles α , β , γ , and δ are displayed in blue. Fixed planes of the amide and urea moieties are indicated with black boxes.

peptide **11a** shows the most pronounced aggregation. Changing the stereochemistry from *all*-(L) to (D)-*alt*-(L) leads to a significantly reduced aggregation of the peptide by a factor of more than 3.¹⁹ Replacing two amide bonds of the natural peptide by one ester-*alt*-urea fragment lowers the aggregation tendency of the naturally configured compound **10a** by a factor of more than 2 (in comparison to **11a**). Within the partial ester-urea series, a change of stereochemistry from *all*-(L) to (D)-*alt*-(L) (**10a** \rightarrow **10b**) again leads to a notable, yet less pronounced drop of aggregation by a factor of roughly 1.5. Finally, substituting all amide bonds with alternating ester and urea moieties leads to a further, but weak decrease of aggregation (by a factor of 1.3, comparing **7a** with **10a**). Importantly, within the complete ester-*alt*-urea series, stereochemical variation has negligible influence on aggregation. Therefore, replacing dipeptide units by an ester-*alt*-urea isostere not only reduces the intrinsic aggregation tendency, but also decreases the influence of stereochemistry on the aggregation behavior of the corresponding oligomer.

As no detailed structural data are available at the moment, a discussion of these results is rather speculative. However, assuming a β -sheet-type aggregate²⁰ structure for all compounds, the different proton shifts have to result from intrinsic strengths of the different hydrogen bonds (amide vs urea) and from different steric interactions of the side chain residues. The *all*-(L)-configured compounds should experience much weaker steric repulsion in this assumed aggregate structure, resulting in stronger association as

compared to the (D)-*alt*-(L)-configured compounds. A potential explanation for the significantly reduced influence of the configuration on the observed proton shift with increasing amount of ester-*alt*-urea moieties involves commensurability of hydrogen bonding donor and acceptor sites as well as rotational stiffness of the backbones (Figure 7). The conformational space of the peptide backbone is governed by only two angles ϕ and ψ (Ramachandran diagram), since the preferred *anti*-conformation of the amide bond fixes this angle to 180°. This limited rotational freedom of the peptide backbone may inhibit the formation of a structure with reduced steric interaction, which is still able to associate in a sheet-type structure. This could explain the notable different aggregation behavior for *all*-(L)- and (D)-*alt*-(L)-peptides. The major difference between the peptide and the ester-*alt*-urea structures is the enhanced rotational freedom of the backbone. By incorporating the β -amino alcohol as well as the ester units, four additional variable rotational angles (α , β , γ , and δ) are introduced and significantly increase backbone flexibility. This could explain the largely reduced aggregation tendency in the partial and exclusive ester-urea series due to a lower degree of preorganization of the backbone on the one hand, and the vanishing influence of monomer configuration (stereochemistry) on association on the other hand.

Conclusion

The ester-urea motif was incorporated into the peptide backbone to replace two adjacent amide residues, giving rise to two new peptide-mimicking scaffolds with either 50% or 100% ester-urea content. Furthermore, the stereochemistry was varied between *all*-(L) and (D)-*alt*-(L). The synthesis of different short oligomers, i.e., tetramers **7a/7b** and **10a/10b**, was readily accomplished by using ester as well as amide couplings to key urea building blocks **3a/3b**. After full characterization, the thus prepared peptide mimics were investigated with regard to their aggregation behavior in organic solution by means of concentration-dependent NMR spectroscopy. It turns out that the naturally occurring peptide scaffold shows the largest association tendency and also the largest discrimination is observed between the *all*-(L) and (D)-*alt*-(L) stereoisomers. Increasing incorporation of the ester-urea motif decreases the aggregation tendency and also the stereochemical differentiation becomes less pronounced and finally vanishes at the complete ester-urea series.

Our findings point to some important structural details in peptides and re-emphasize key requirements for (their) efficient association processes. Although, the urea moiety itself is rigid and engages in rather strong hydrogen bonding interactions, introduction of the ester reduces the number of interacting sites and furthermore increases conformational flexibility due to employed β -amino alcohol unit and the ester linkage. Both of these effects significantly lower the overall association tendency and ability of stereochemical differentiation of the backbone configuration. Clearly, the correct orientation of *amide* bonds is most suited to mediate association. On the one hand, amides offer the advantage to display an equal number of hydrogen bonding donating and accepting sites to maximize the number of interacting units on both faces of the backbone following the principles of

(19) This factor is based on the *average* chemical shift differences of all participating protons (numbered in Figures 5–7). Due to the limited concentration range and the significant deviations of the chemical shift differences of the individual protons, no association constants were calculated as these individual or average values would have rather limited meaning. True association constants necessitate, for example, in depth isothermal titration calorimetry measurements.

(20) (a) Sewald, N.; Jakubke, H.-D. *Peptides: Chemistry and Biology*; Wiley-VCH: Weinheim, Germany, 2003. (b) Quinkert, G.; Egert, E.; Griesinger, C. *Aspects of Organic Chemistry: Structure*; VHCA, Basel, Switzerland, 1996.

commensurability and multivalency.²¹ On the other hand, they are conformationally restricted and hence their preorganization leads to a favorable (or at least not negative) entropic contribution to association.²² Interestingly, association of the peptide is much more dependent on the backbone configuration (as compared to the ester-ureas), demonstrating the large effect of stereochemistry on backbone conformation and the ability of using side chain interactions to tune peptide association. The obtained structure-aggregation relationships illustrate the emergence and particular strength of β -sheet-type aggregation in peptides and proteins²³ and point to potential ways to weaken their association processes by using β -sheet breaking peptide-mimics²⁴ and to design improved small molecule gelators.⁸

Future work will be focused on detailed investigations elucidating the structure of the formed aggregates and their superstructures, i.e., fibers/gels, as well as determination of the association constants by isothermal titration calorimetry. Further synthetic work will be targeting the design of water-soluble peptide mimics with incorporated photo-switchable units to externally control self-assembly.²⁵

Experimental Section

The synthesis and characterization data of key compounds are provided below. For further details on general methods, experimental procedures, and characterization data, including copies of spectral data, consult the Supporting Information.

(L)-Leucinol-urea-(L)-leucine-Bn (3a). (L)-Leu-Bn **1a** (1.01 g, 3.00 mmol) and NEt_3 (0.42 mL, 3.00 mmol) were dissolved in CH_2Cl_2 (20 mL) and added to a solution of carbonyldiimidazole (CDI; 0.97 g, 6.00 mmol) in CH_2Cl_2 (50 mL) at 0 °C within 1 h. After being stirred at 0 °C for 1 h, the mixture was allowed to warm to room temperature and stirred for 1 h. The reaction mixture was extracted with water (2 × 100 mL) and brine (1 × 100 mL). The organic layer was dried over MgSO_4 , filtered, and evaporated in vacuo to give the intermediate imidazole-urea. L-Leucinol **2** (0.35 g, 3.00 mmol), dissolved in CH_2Cl_2 (100 mL), was cooled to 0 °C and the intermediate imidazole-urea, dissolved in CH_2Cl_2 (20 mL), was added within 20 min. The mixture was allowed to warm to room temperature and stirred for 16 h. The reaction mixture was washed with water (1 × 50 mL), 1 M aqueous citric acid solution (1 × 50 mL), water (1 × 50 mL), saturated aqueous NaHCO_3 solution (1 × 50 mL), water (1 × 50 mL), and brine (1 × 50 mL). The organic layer was dried over MgSO_4 , filtered, and evaporated in vacuo to give 1.16 g of the crude product, which was purified via silica column chromatography (eluent: PE:EA = 1:1). The second column gave 900 mg (82%) of pure product as colorless crystals. R_f 0.50

(PE: EA = 2: 8). HPLC (2 × 150 mm Luna Phenyl-Hexyl 3 μm , acetonitrile (AN):water, grad: 5 → 95 vol % AN): t_R = 18.57 min (> 99.0% peak area). ^1H NMR (300 MHz, CDCl_3 , 20 °C): δ 7.36–7.31 (m, 5 H, C^{11-13}H), 5.99–5.94 (m, 1 H, N^6H), 5.59–5.54 (m, 1 H, N^4H), 5.19–5.07 (m, 2 H, C^9H_2), 4.48–4.42 (m, 1 H, C^7H), 4.00 (br s, 1 H, O^1H), 3.76–3.71 (m, 1 H, C^3H), 3.58 (dd, $^2J(\text{H},\text{H}) = 11.0$ Hz, $^3J(\text{H},\text{H}) = 3.4$ Hz, 1 H, $1\text{C}^2\text{H}_2$), 3.46 (dd, $^2J(\text{H},\text{H}) = 11.0$ Hz, $^3J(\text{H},\text{H}) = 6.5$ Hz, 1 H, $1\text{C}^2\text{H}_2$), 1.72–1.46 (m, 4 H, C^{14}H_2 , C^{17}H_2), 1.44–1.23 (m, 2 H, C^{15}H , C^{18}H), 0.93–0.87 (m, 12 H, 2 C^{16}H_3 , 2 C^{19}H_3). ^{13}C NMR (CDCl_3): δ 174.6, 159.2, 135.5, 128.5, 128.3, 128.0, 66.9, 66.8, 52.0, 51.1, 41.5, 40.5, 24.81, 24.78, 23.1, 22.8, 22.2, 22.0. HR-ESI-MS: m/z 365.2435 (calcd 365.2443 for $\text{C}_{20}\text{H}_{32}\text{N}_2\text{O}_4 + 1\text{H}^+$).

(L)-Leucinol-urea-(D)-leucine-Bn (3b). (D)-Leu-Bn **1a** (13.08 g, 39.00 mmol) and NEt_3 (7.59 mL, 54.60 mmol) were dissolved in CH_2Cl_2 (100 mL) and added to a solution of CDI (12.65 g, 78.00 mmol) in CH_2Cl_2 (400 mL) at 0 °C within 1 h. After addition, the mixture was stirred for 1 h at 0 °C, then for 2 h at room temperature. The reaction mixture was extracted with water (2 × 100 mL). The organic layer was dried over MgSO_4 , filtered, and evaporated in vacuo to give the intermediate imidazole-urea. (L)-Leucinol **2** (4.80 g, 40.95 mmol), dissolved in CH_2Cl_2 (400 mL), was cooled to 0 °C and the intermediate imidazole-urea, dissolved in CH_2Cl_2 (100 mL), was added within 1 h. The mixture was allowed to warm to room temperature and stirred for 16 h. Water was added to the reaction mixture and the biphasic system was stirred for 30 min. After phase separation, the organic layer was evaporated in vacuo and CH_2Cl_2 was replaced by EA. The organic layer was washed with water (2 × 100 mL), 1 M aqueous citric acid solution (2 × 50 mL), water (1 × 50 mL), saturated aqueous NaHCO_3 solution (1 × 50 mL), water (1 × 50 mL), and brine (1 × 50 mL). The organic layer was dried over MgSO_4 , filtered, and evaporated in vacuo to give the crude product, which was purified via recrystallization from PE: CH_2Cl_2 to give 12.51 g (88%) of pure **3b** as colorless crystals. R_f 0.50 (PE: EA = 2: 8). HPLC (2 × 150 mm Luna Phenyl-Hexyl 3 μm , acetonitrile: water, grad: 5 → 95 vol % AN): t_R = 18.82 min (> 99.0% peak area). ^1H NMR (300 MHz, CDCl_3 , 20 °C): δ 7.34–7.30 (m, 5 H, C^{11-13}H), 6.01 (d, $^3J(\text{H},\text{H}) = 6.7$ Hz, 1 H, N^6H), 5.66–5.60 (m, 1 H, N^4H), 5.20–5.05 (m, 2 H, C^9H_2), 4.56–4.44 (m, 1 H, C^7H), 4.17 (br s, 1 H, O^1H), 3.85–3.70 (m, 1 H, C^3H), 3.60 (dd, $^2J(\text{H},\text{H}) = 11.0$ Hz, $^3J(\text{H},\text{H}) = 3.2$ Hz, 1 H, $1\text{C}^2\text{H}_2$), 3.41 (dd, $^2J(\text{H},\text{H}) = 11.0$ Hz, $^3J(\text{H},\text{H}) = 5.8$ Hz, 1 H, $1\text{C}^2\text{H}_2$), 1.79–1.46 (m, 4 H, C^{14}H_2 , C^{17}H_2), 1.44–1.17 (m, 2 H, C^{15}H , C^{18}H), 0.93–0.87 (m, 12 H, C^{16}H_3 , C^{19}H_3). ^{13}C NMR (CDCl_3): δ 175.2, 158.9, 135.4, 128.5, 128.2, 128.0, 66.9, 66.1, 51.8, 50.5, 41.5, 40.8, 24.8, 23.0, 22.8, 22.3, 21.9. HR-ESI-MS: m/z 365.2456 (calcd 365.2440 for $\text{C}_{20}\text{H}_{33}\text{N}_2\text{O}_4 + 1\text{H}^+$).

TBDPS-(L)-leucinol-urea-(L)-leucine-Bn (4a). **3a** (5.45 g, 14.95 mmol), imidazole (2.04 g, 29.90 mmol), and TBDPS-Cl (0.17 g, 1.12 mmol) were dissolved in DMF (50 mL) and the mixture was stirred for 3 h. The solution was poured on ice, and the aqueous layer was extracted with Et_2O , dried over MgSO_4 , and evaporated in vacuo. The crude product was purified via silica column chromatography (eluent: PE:EA = 10:1) to give 7.38 g (yield: 81%) of the desired product. An NMR sample in CDCl_3 showed decomposition but the pure product could be stored in a freezer without decomposition. R_f 0.70 (PE:EA = 10:1). UPLC (2.1 × 100 mm BEH Phenyl 1.7 μm , acetonitrile: water, grad: 40 → 95 vol % AN): t_R = 4.60 min (86.1% peak area). ^1H NMR (300 MHz, CD_2Cl_2 , 20 °C): δ 7.72–7.56 (m, 4 H, C^{19}H), 7.38–7.25 (m, 11 H, C^{12-14}H , C^{20-21}H), 5.10 (s, 2 H, C^{10}H_2), 4.67 (d, $^3J(\text{H},\text{H}) = 8.7$ Hz, 1 H, N^7H), 4.46 (d, $^3J(\text{H},\text{H}) = 9.1$ Hz, 1 H, N^5H), 4.43–4.34 (m, 1 H, C^5H), 3.84–3.71 (m, 1 H, C^4H), 3.65–3.51 (m, 1 H, C^3H_2), 1.67–1.25 (m, 6 H, 2 C^{15}H_2 , 2 C^{16}H), 1.00 (s, 9 H, 3 C^{17}H_3), 0.91–0.74 (m, 12 H, 4 C^{17}H_3). ^{13}C

(21) (a) Mammen, M.; Choi, S.-K.; Whitesides, G. M. *Angew. Chem., Int. Ed.* **1998**, *37*, 2754. (b) Lundquist, J. L.; Toone, E. J. *Chem. Rev.* **2002**, *102*, 555.

(22) (a) Page, M. L.; Jencks, W. P. *Proc. Natl. Acad. Sci.* **1971**, *68*, 1678. For a review, see: (b) Jencks, W. P. *Adv. Enzymol.* **1975**, *43*, 219. A theoretical treatment is given in: (c) Mammen, M.; Shakhovich, E. I.; Whitesides, G. M. *J. Org. Chem.* **1998**, *63*, 3168.

(23) (a) Rauk, A. *Chem. Soc. Rev.* **2009**, *38*, 2698. (b) Hamley, I. W. *Angew. Chem., Int. Ed.* **2007**, *46*, 8128. (c) Chiti, F.; Dobson, C. M. *Annu. Rev. Biochem.* **2006**, *75*, 333. (d) *Misbehaving Proteins: Protein (Mis)Folding, Aggregation, and Stability*, Tsai, A.; Murphy, R., Ed.; Springer: Berlin, Germany, 2006.

(24) For recent examples, see: (a) Coelho, M.; Rocha, S. *Biochem. Biophys. Res. Commun.* **2009**, *380*, 397. (b) Kim, Y. S.; Lim, D.; Kim, J. Y.; Kang, S. J.; Kim, Y.-H.; Im, H. *Biochem. Biophys. Res. Commun.* **2009**, *387*, 682. For overviews, see: (c) Adessi, C.; Soto, C. *Drug Dev. Res.* **2002**, *56*, 184. (d) Mason, J. M.; Kokkonis, N.; Stott, K.; Doig, A. J. *Curr. Opin. Struct. Biol.* **2003**, *13*, 526.

(25) For a highlight, see: Hecht, S. *Small* **2005**, *1*, 26 and references cited therein.

NMR (CD₂Cl₂): δ 174.0, 156.9, 135.9, 135.6, 133.6, 133.5, 129.7, 129.7, 128.5, 128.2, 128.0, 127.7, 66.6, 66.5, 51.8, 49.8, 41.8, 41.2, 26.7, 24.8, 24.7, 22.8, 22.6, 21.6, 20.8, 19.2. HR-ESI-MS: m/z 603.3449 (calcd 603.3618 for C₃₆H₅₁N₂O₄Si₁ + 1 H⁺).

TBDPS-(L)-leucinol-urea-(D)-leucine-Bn (4b). **3b** (5.45 g, 14.95 mmol), imidazole (2.04 g, 29.90 mmol), and TBDPS-Cl (0.17 g, 1.12 mmol) were dissolved in DMF (50 mL) and the mixture was stirred for 3 h. The solution was poured on ice, and the aqueous layer was extracted with Et₂O, dried over MgSO₄, and evaporated in vacuo. The crude product was purified via silica column chromatography (eluent: PE:EA = 10:1) to give 7.63 g (yield: 85%) of the desired product. An NMR sample in CDCl₃ showed decomposition but the pure product could be stored in a freezer without decomposition. R_f 0.70 (PE:EA = 10:1). HPLC (2 × 150 mm Luna Phenyl-Hexyl 3 μ m, acetonitrile:water, grad: 40 → 95 vol % AN): t_R = 20.02 min (> 99.0% peak area). ¹H NMR (300 MHz, CD₃CN, 20 °C) δ 7.70–7.67 (m, 4 H, C¹⁹H), 7.45–7.34 (m, 11 H, C^{12–14}H, 2 C^{20–21}H), 5.31 (d, ³J(H,H) = 8.3 Hz, 1 H, N⁷H), 5.12 (s, 2 H, C¹⁰H₂), 5.05 (d, ³J(H,H) = 8.3 Hz, 1 H, N⁵H), 4.39–4.31 (m, 1 H, C⁵H), 3.86–3.82 (m, 1 H, C⁴H), 3.61–3.58 (m, 1 H, C³H₂), 1.66–1.37 (m, 6 H, 2 C¹⁵H₂, 2 C¹⁶H), 1.06 (s, 9 H, 3 C¹H₃), 0.98–0.83 (m, 12 H, 4 C¹⁷H₃). ¹³C NMR (CD₃CN): δ 174.6, 158.2, 137.3, 136.4, 134.5, 134.5, 130.8, 130.7, 129.4, 129.0, 128.9, 128.8, 67.5, 68.0, 52.6, 50.3, 42.1, 41.8, 27.2, 25.6, 25.6, 23.5, 23.1, 22.6, 22.1, 19.8. HR-ESI-MS: m/z 603.3604 (calcd 603.3613 for C₃₆H₅₁N₂O₄Si₁ + 1 H⁺).

TBDPS-(L)-leucinol-urea-(L)-leucine (5a). To a solution of **4a** (1.00 g, 1.60 mmol) and 50 mL of ethanol was added Pd/C (10 wt %, 120 mg) and the solution was stirred under hydrogen atmosphere at room temperature for 12 h. The reaction mixture was filtered and evaporated in vacuo to give the desired product in 55% yield (0.47 g). R_f 0.50 (CH₂Cl₂:MeOH = 100:5). UPLC (2.1 × 100 mm BEH Phenyl 1.7 μ m, acetonitrile:water, grad: 40 → 95 vol % AN): t_R = 4.86 min (68.0% peak area). ¹H NMR (300 MHz, CD₂Cl₂, 20 °C): δ 7.71–7.65 (m, 4 H, C¹⁵H), 7.50–7.37 (m, 6 H, C^{16–17}H), 5.34–5.24 (m, 1 H, N⁷H), 5.20–5.07 (m, 1 H, N⁵H), 4.30–4.20 (m, 1 H, C⁵H), 3.90–3.75 (m, 1 H, C⁴H), 3.71–3.59 (m, 1 H, C³H₂), 1.81–1.31 (m, 6 H, 2 C¹¹H₂, 2 C¹²H), 1.09 (s, 9 H, 3 C¹H₃), 1.04–0.88 (m, 12 H, 4 C¹³H₃). ¹³C NMR (CD₂Cl₂): δ 175.7, 159.0, 135.6, 133.4, 133.2, 129.8, 128.5, 128.0, 127.7, 66.7, 60.3, 40.8, 40.4, 26.7, 24.72, 24.68, 22.77, 22.76, 22.0, 21.5, 20.0. HR-ESI-MS: m/z 513.3134 (calcd 513.3143 for C₂₉H₄₅N₂O₄Si₁ + 1 H⁺).

TBDPS-(L)-leucinol-urea-(D)-leucine (5b). To a solution of **4b** (1.00 g, 1.60 mmol) in 50 mL of ethanol was added Pd/C (10 wt %, 120 mg) and the solution was stirred under hydrogen atmosphere at room temperature for 12 h. The reaction mixture was filtered and evaporated in vacuo to give the desired product in 58% yield (0.49 g). R_f 0.50 (CH₂Cl₂:MeOH = 100:5). HPLC (2 × 150 mm Luna Phenyl-Hexyl 3 μ m, acetonitrile:water, grad: 40 → 95 vol % AN): t_R = 17.18 min (> 99.9% peak area). ¹H NMR (300 MHz, CD₃CN, 20 °C): δ 7.70–7.66 (m, 4 H, C¹⁵H), 7.45–7.42 (m, 6 H, C^{16–17}H), 5.42 (d, ³J(H,H) = 7.1 Hz, 1 H, N⁷H), 5.29 (d, ³J(H,H) = 8.3 Hz, 1 H, N⁵H), 4.20–4.16 (m, 1 H, C⁵H), 3.80–3.77 (m, 1 H, C⁴H), 3.63–3.60 (m, 1 H, C³H₂), 1.81–1.31 (m, 6 H, 2 C¹¹H₂, 2 C¹²H), 1.06 (s, 9 H, 3 C¹H₃), 0.91–0.86 (m, 12 H, 4 C¹³H₃). ¹³C NMR (CD₃CN): δ 174.5, 158.7, 135.5, 129.8, 129.8, 127.8, 66.4, 52.1, 49.7, 40.6, 40.3, 26.3, 24.6, 24.6, 22.5, 22.2, 21.6, 21.0, 18.9. HR-ESI-MS: m/z 513.3134 (calcd 513.3143 for C₂₉H₄₅N₂O₄Si₁ + 1 H⁺).

TBDPS-[(L)-leucinol-urea-(L)-leucine]₂-Bn (6a). **3a** (1.50 g, 4.12 mmol), **5a** (2.32 g, 4.53 mmol), and DMAP (0.50 g, 4.12 mmol) were dissolved in CH₂Cl₂ (100 mL) and the mixture was cooled to 0 °C. EDC (1.74 g, 9.05 mmol), dissolved in CH₂Cl₂ (5 mL), was added slowly. The reaction mixture was allowed to warm to room temperature, stirred for 5 h, and evaporated in

vacuo. The residue was purified via silica column chromatography (eluent: PE:EA = 4:2) to give 1.95 g (yield: 55%) of the desired product. R_f 0.50 (PE:EA = 2:1). UPLC (2.1 × 100 mm BEH Phenyl 1.7 μ m, acetonitrile:water, grad: 40 → 95 vol % AN): t_R = 5.61 min (84.0% peak area). ¹H NMR (300 MHz, CDCl₃, 20 °C): δ 7.67–7.62 (m, 4 H, C²⁶H), 7.43–7.28 (m, 10 H, C^{19–21}H, C^{27–28}H), 5.42–5.26 (m, 2 H, 2 NH), 5.15–4.90 (m, 3 H, C¹⁷H₂, NH), 4.73–4.60 (m, 1 H, NH), 4.57–4.42 (m, 2 H, C⁸H, C¹⁵H), 4.35–4.24 (m, 1 H, C¹¹H), 4.07–3.93 (m, 1 H, C⁴H), 3.95–3.57 (m, 4 H, C³H₂, C¹⁰H₂), 1.73–1.24 (m, 12 H, 4 C²²H₂, 4 C²³H), 1.07 (s, 9 H, 3 C¹H₃), 0.98–0.82 (m, 24 H, 8 C²⁴H₃). ¹³C NMR (CDCl₃): δ 174.2, 157.8, 157.3, 135.6, 133.4, 133.3, 129.84, 129.80, 128.5, 128.2, 128.1, 127.8, 66.9, 66.7, 50.6, 52.2, 51.6, 47.3, 42.3, 41.4, 41.2, 41.0, 26.9, 24.76, 24.72, 22.9, 22.8, 22.7, 22.5, 22.4, 22.1, 19.3, 14.9. HR-ESI-MS: m/z 859.5394 (calcd 859.5400 for C₄₉H₇₅N₄O₇Si₁ + 1 H⁺).

TBDPS-[(L)-leucinol-urea-(D)-leucine]₂-Bn (6b). **3b** (1.50 g, 4.12 mmol), **5b** (2.32 g, 4.53 mmol), and DMAP (0.50 g, 4.12 mmol) were dissolved in CH₂Cl₂ (100 mL) and the mixture was cooled to 0 °C. EDC (1.74 g, 9.05 mmol), dissolved in CH₂Cl₂ (5 mL), was added slowly. The reaction mixture was allowed to warm to room temperature, stirred for 5 h, and evaporated in vacuo. The residue was purified via silica column chromatography (eluent: PE:EA = 4:2) to give 1.88 g (yield: 53%) of the desired product. R_f 0.50 (PE:EA = 2:1). HPLC (2 × 150 mm Luna Phenyl-Hexyl 3 μ m, acetonitrile:water, grad: 70 → 95 vol % AN): t_R = 15.75 min (95.8% peak area). ¹H NMR (300 MHz, CD₃CN, 20 °C): δ 7.70–7.64 (m, 4 H, C²⁶H), 7.45–7.37 (m, 10 H, C^{19–21}H, C^{27–28}H), 5.43 (d, ³J(H,H) = 7.2 Hz, 1 H, NH), 5.32 (d, ³J(H,H) = 7.6 Hz, 1 H, NH), 5.23–5.04 (m, 4 H, C¹⁷H₂, 2 NH), 4.35–4.12 (m, 3 H, C⁸H, C¹¹H, C¹⁵H), 3.95–3.76 (m, 3 H, C⁴H, C¹⁰H₂), 3.64–3.51 (m, 1 H, C³H₂), 1.72–1.16 (m, 12 H, 4 C²²H₂, 4 C²³H), 1.04 (s, 9 H, 3 C¹H₃), 0.94–0.74 (m, 24 H, 8 C²⁴H₃). ¹³C NMR (CD₃CN): δ 173.7, 173.3, 157.8, 157.6, 136.3, 135.5, 133.5, 133.4, 129.82, 129.79, 128.5, 128.1, 127.9, 127.8, 117.3, 66.8, 66.5, 66.2, 52.1, 51.7, 49.4, 47.0, 41.05, 40.98, 40.9, 40.7, 26.3, 24.6, 24.6, 24.5, 22.6, 22.4, 22.2, 21.6, 21.4, 21.15, 21.09, 18.9. HR-ESI-MS: m/z 859.5402 (calcd 859.5400 for C₄₉H₇₅N₄O₇Si₁ + 1 H⁺).

[(L)-Leucinol-urea-(L)-leucine]₂-Bn (7a). **6a** (0.22 g, 0.26 mmol) was dissolved in acetonitrile (10 mL) and HF (0.10 mL) was added. The reaction mixture was stirred for 2 h. K₂CO₃ was added, and the solution was filtered and evaporated in vacuo. The residue was purified via silica column chromatography (eluent: CH₂Cl₂:MeOH = 10:1) to give 0.15 g (yield: 94%) of the desired product. R_f 0.50 (CH₂Cl₂:MeOH = 10:1). UPLC (2.1 × 100 mm BEH Phenyl 1.7 μ m, acetonitrile:water, grad: 40 → 95 vol % AN): 3.45 min (> 99.9% peak area). ¹H NMR (400 MHz, CD₂Cl₂, 20 °C): δ 7.40–7.29 (m, 5 H, C^{18–20}H), 5.46 (br s, 1 H, N⁶H), 5.35 (d, ³J(H,H) = 8.2 Hz, 1 H, N¹³H), 5.27 (d, ³J(H,H) = 9.0 Hz, 1 H, N¹¹H), 5.12 (s, 2 H, C¹⁶H₂), 4.78 (d, ³J(H,H) = 7.5 Hz, 1 H, N⁴H), 4.48 (dd, ²J(H,H) = 10.8 Hz, ³J(H,H) = 3.4 Hz, 1 H, 1 C⁹H₂), 4.41 (dt, ³J(H,H) = 8.5 Hz, ³J(H,H) = 6.0 Hz, 1 H, C¹⁴H), 4.16 (dt, ³J(H,H) = 8.5 Hz, ³J(H,H) = 6.0 Hz, 1 H, C⁷H), 4.02–3.92 (m, 1 H, C¹⁰H), 3.81 (dd, ²J(H,H) = 10.8 Hz, ³J(H,H) = 4.0 Hz, 1 H, 1 C⁹H₂), 3.70–3.61 (m, 1 H, C³H), 3.60–3.54 (m, 1 H, 1 C²H₂), 3.47–3.34 (m, 2 H, 1 C²H₂, O₁H), 1.74–1.19 (m, 12 H, 4 C²¹H₂, 4 C²²H), 0.97–0.87 (m, 24 H, 8 C²³H₃). ¹³C NMR (CD₂Cl₂): δ 174.4, 174.1, 159.3, 157.1, 135.8, 128.5, 128.2, 128.0, 67.2, 66.7, 52.4, 52.8, 47.1, 41.9, 41.5, 41.1, 40.8, 40.3, 24.9, 24.8, 24.1, 22.9, 22.6, 22.54, 22.52, 22.1, 22.0, 21.9, 21.8. HR-ESI-MS: m/z 621.4229 (calcd 621.4222 for C₃₃H₅₆N₄O₇ + 1 H⁺).

[(L)-Leucinol-urea-(D)-leucine]₂-Bn (7b). **6b** (0.22 g, 0.26 mmol) was dissolved in acetonitrile (10 mL) and HF (0.10 mL) was added. The reaction mixture was stirred for 2 h. K₂CO₃ was added, and the solution was filtered and evaporated in vacuo. The residue was purified via silica column chromatography

(eluent: CH₂Cl₂:MeOH = 10:1) to give 0.16 g (yield: 98%) of the desired product. *R_f* 0.50 (CH₂Cl₂:MeOH = 10:1). HPLC (2 × 150 mm Luna Phenyl-Hexyl 3 μm, acetonitrile:water, grad: 40 → 95 vol% AN): *t_R* = 14.80 min (>99.9% peak area). ¹H NMR (400 MHz, CD₂Cl₂, 20 °C): δ 7.40–7.31 (m, 5 H, C^{18–20}H), 5.16 (d, ³*J*(H,H) = 7.8 Hz, 1 H, N¹³H), 5.11 (d, ³*J*(H,H) = 8.2 Hz, 1 H, N⁶H), 5.15 (dd, ²*J*(H,H) = 51.3 Hz, ³*J*(H,H) = 12.4 Hz, 2 H, C¹⁶H₂), 4.89 (d, ³*J*(H,H) = 8.0 Hz, 1 H, N⁴H), 4.84 (d, ³*J*(H,H) = 9.4 Hz, 1 H, N¹¹H), 4.39–4.31 (m, 2 H, C⁷H, C¹⁴H), 4.25–4.20 (m, 1 H, O¹H), 4.13–4.02 (m, 2 H, 1 C⁹H₂, C¹⁰H), 3.89–3.81 (m, 2 H, C³H, 1 C⁹H₂), 3.67–3.61 (m, 1 H, 1 C²H₂), 3.39–3.32 (m, 1 H, 1 C²H₂), 1.81–1.18 (m, 12 H, 4 C²¹H₂, 4 C²²H), 0.97–0.87 (m, 24 H, 8 C²³H₃). ¹³C NMR (CD₂Cl₂): δ 174.7, 173.4, 159.6, 158.1, 135.6, 128.5, 128.0, 67.9, 66.9, 66.6, 53.8, 53.4, 53.1, 50.7, 47.2, 40.84, 40.79, 40.6, 40.5, 24.8, 24.7, 22.9, 22.8, 22.7, 22.6, 22.1, 21.8. HR-ESI-MS: *m/z* 621.4230 (calcd 621.4222 for C₃₃H₅₆N₄O₇ + 1 H⁺).

Boc-(L)-leucine-ester-(L)-leucinol-urea-(L)-leucine-Bn (8a). 3a (1.09 g, 3.00 mmol), Boc-(L)-Leu-OH (0.90 g, 3.60 mmol), and DMAP (0.37 g, 3.00 mmol) were dissolved in CH₂Cl₂ (250 mL) and the mixture was cooled to 0 °C. To the cold solution was added EDC (1.73 g, 1.80 mmol). The solution was allowed to warm to room temperature and stirred for 2 h. The reaction mixture was quenched by the addition of silica gel. After the mixture was stirred for 2 h, the solvent was evaporated in vacuo on a column and purified via silica column chromatography (eluent: Et₂O). The crude product (1.74 g) was purified via silica column chromatography (eluent: PE:EA) to remove more un-polar substances to give 1.72 g of pure 7a. *R_f* 0.28 (PE:EA 4:1). HPLC (2 × 150 mm Luna Phenyl-Hexyl 3 μm, acetonitrile:water, grad: 5 → 95 vol % AN): *t_R* = 23.07 min (>99.0% peak area). ¹H NMR (300 MHz, CD₃OD, 20 °C): δ 7.36–7.30 (m, 5 H, C^{16–18}H), 5.14 (dd, *J*(H,H) = 12.4 Hz, *J*(H,H) = 13.5 Hz, 2 H, C¹⁴H₂), 4.35 (dd, *J*(H,H) = 5.8 Hz, *J*(H,H) = 9.1 Hz, 1 H, C⁵H or C¹²H), 4.17 (t, ³*J*(H,H) = 7.5 Hz, 1 H, C⁵H or C¹²H or 1 C⁷H₂), 4.06–3.97 (m, 3 H, 1 C⁷H₂, C⁸H, 1 C⁷H₂ or C⁵H or C¹²H), 1.78–1.24 (m, 18 H, 3 C¹H₃, 3 C¹⁹H₂, 3 C²⁰H), 0.97–0.89 (m, 18 H, 6 C²¹H₃). ¹³C NMR (CD₃OD): δ 175.1, 174.8, 159.9, 158.1, 135.2, 129.5, 129.20, 129.17, 80.5, 68.3, 67.6, 53.4, 53.0, 48.1, 42.2, 42.0, 41.6, 28.7, 25.9, 25.9, 25.7, 23.6, 23.3, 23.2, 22.4, 22.2, 21.9. HR-ESI-MS: *m/z* 578.3797 (calcd 578.3805 for C₃₁H₅₁N₃O₇ + 1 H⁺).

Boc-(D)-leucine-ester-(L)-leucinol-urea-(D)-leucine-Bn (8b). 3b (1.09 g, 3.00 mmol), Boc-(D)-Leu-OH (0.90 g, 3.60 mmol), and DMAP (0.37 g, 3.00 mmol) were dissolved in CH₂Cl₂ (250 mL) and cooled to 0 °C. To the cold solution was added EDC (1.73 g, 1.80 mmol). The solution was allowed to warm to room temperature and stirred for 5 h. The reaction mixture was quenched by the addition of silica gel. After the mixture was stirred for 1 h, the solvent was evaporated in vacuo. The residue was purified via silica column chromatography (eluent: Et₂O). The crude product (1.80 g) was recrystallized from PE:CH₂Cl₂ to give 1.73 g of pure 8b in quantitative yield. *R_f* 0.30 (PE:EA = 4:1). HPLC (2 × 150 mm Luna Phenyl-Hexyl 3 μm, acetonitrile:water, grad: 5 → 95 vol % AN): *t_R* = 23.07 min (>99.0% peak area). ¹H NMR (300 MHz, CD₃OD, 20 °C): δ 7.36–7.29 (m, 5 H, C^{16–18}H), 5.14 (dd, *J*(H,H) = 12.3 Hz, *J*(H,H) = 25.1 Hz, 2 H, C¹⁴H₂), 4.38 (dd, *J*(H,H) = 5.6 Hz, *J*(H,H) = 9.1 Hz, 1 H, C⁵H or C¹²H), 4.18 (t, ³*J*(H,H) = 7.5 Hz, 1 H, C⁵H or C¹²H or 1 C⁷H₂), 4.08–4.00 (m, 3 H, 1 C⁷H₂, C⁸H, 1 C⁷H₂ or C⁵H or C¹²H), 1.78–1.26 (m, 18 H, 3 C¹H₃, 3 C¹⁹H₂, 3 C²⁰H), 0.95–0.90 (m, 18 H, 6 C²¹H₃). ¹³C NMR (CD₃OD): δ 174.9, 174.6, 159.8, 158.0, 137.2, 129.5, 129.2, 129.2, 80.3, 68.3, 67.6, 53.5, 52.8, 48.1, 42.3, 41.9, 41.3, 28.8, 25.9, 25.84, 25.77, 23.6, 23.3, 23.3, 22.4, 22.1, 21.8. HR-ESI-MS: *m/z* 578.3817 (calcd 578.3805 for C₃₁H₅₁N₃O₇ + 1 H⁺).

Boc-(L)-leucine-ester-(L)-leucinol-urea-(L)-leucine (9a). To a solution of 8a (1.73 g, 3.00 mmol) in 50 mL of ethyl acetate

was added Pd/C (10 wt %, 170 mg) and the solution was stirred under 6 bar hydrogen-pressure atmosphere at room temperature for 1 h. The reaction mixture was filtered and evaporated in vacuo to give 1.45 g of the desired product (99% yield). *R_f* 0.40 (Et₂O). HPLC (2 × 150 mm Luna Phenyl-Hexyl 3 μm, acetonitrile:water, grad: 5 → 95 vol % AN): *t_R* = 19.84 min (>99.0% peak area). ¹H NMR (300 MHz, CD₃OD, 20 °C): δ 4.29 (dd, *J*(H,H) = 5.2 Hz, *J*(H,H) = 9.3 Hz, 1 H, C⁵H or C¹²H), 4.17 (t, ³*J*(H,H) = 7.5 Hz, 1 H, C⁵H or C¹²H or 1 C⁷H₂), 4.11–3.96 (m, 3 H, 1 C⁷H₂, C⁸H, 1 C⁷H₂ or C⁵H or C¹²H), 1.83–1.25 (m, 18 H, 3 C¹H₃, 3 C¹⁵H₂, 3 C²⁶H), 0.97–0.91 (m, 18 H, 6 C¹⁷H₃). ¹³C NMR (CD₃OD): δ 177.2, 174.8, 160.1, 158.1, 80.5, 68.4, 53.5, 52.7, 48.1, 42.6, 42.1, 41.6, 28.8, 26.0, 25.8, 23.6, 23.4, 23.3, 22.5, 22.2, 21.9. HR-ESI-MS: *m/z* 488.3347 (calcd 488.3336 for C₂₄H₄₅N₃O₇ + 1 H⁺).

Boc-(D)-leucine-ester-(L)-leucinol-urea-(D)-leucine (9b). To a solution of 8b (1.73 g, 3.00 mmol) in 50 mL of ethyl acetate was added Pd/C (10 wt %, 170 mg) and the solution was stirred under 6 bar hydrogen-pressure atmosphere at room temperature for 3 h. The reaction mixture was filtered and evaporated in vacuo to give 1.08 g of the desired product (74% yield). *R_f* 0.30 (Et₂O). HPLC (2 × 150 mm Luna Phenyl-Hexyl 3 μm, acetonitrile:water, grad: 5 → 95 vol % AN): *t_R* = 20.15 min (>99.0% peak area). ¹H NMR (300 MHz, CD₃OD, 20 °C): δ 4.32 (dd, *J*(H,H) = 5.1 Hz, *J*(H,H) = 9.3 Hz, 1 H, C⁵H or C¹²H), 4.16 (t, ³*J*(H,H) = 7.5 Hz, 1 H, C⁵H or C¹²H or 1 C⁷H₂), 4.06–4.01 (m, 3 H, 1 C⁷H₂, C⁸H, 1 C⁷H₂ or C⁵H or C¹²H), 1.82–1.25 (m, 18 H, 3 C¹H₃, 3 C¹⁵H₂, 3 C²⁶H), 0.97–0.91 (m, 18 H, 6 C¹⁷H₃). ¹³C NMR (CD₃OD): δ 177.1, 174.7, 159.9, 158.1, 80.4, 68.4, 53.5, 52.6, 48.1, 42.8, 41.9, 41.3, 28.7, 26.0, 25.9, 25.8, 23.6, 23.4, 23.3, 22.4, 22.2, 21.8. HR-ESI-MS: *m/z* 488.3347 (calcd 488.3336 for C₂₄H₄₅N₃O₇ + 1 H⁺).

Boc-(L)-leucine-ester-(L)-leucinol-urea-(L)-leucine-amide-(L)-leucine-Bn (10a). 9a (1.27 g, 2.61 mmol), 1a (0.60 g, 2.70 mmol), and DMAP (0.32 g, 2.61 mmol) were dissolved in CH₂Cl₂ (30 mL) and the mixture was cooled to 0 °C. To the cold solution was added EDC (1.00 g, 5.22 mmol). The solution was allowed to warm to room temperature and stirred for 24 h. The reaction mixture was quenched by the addition of silica gel. After the mixture was stirred for 4 h, the solvent was evaporated in vacuo. The residue was purified via silica column chromatography (eluent: PE:EA = 5:1 to 3:1) to give 1.52 g (84%) of pure 10a. *R_f* 0.34 (PE:EA = 1:1). HPLC (2 × 150 mm Luna Phenyl-Hexyl 3 μm, acetonitrile:water, grad: 5 → 95 vol % AN): *t_R* = 19.84 min (97.0% peak area). ¹H NMR (400 MHz, CD₂Cl₂, 20 °C): δ 7.40–7.30 (m, 5 H, C^{19–21}H), 6.74 (d, ³*J*(H,H) = 7.6 Hz, 1 H, N¹⁴H), 5.13 (dd, *J*(H,H) = 12.8 Hz, *J*(H,H) = 16.6 Hz, 2 H, C¹⁷H₂), 5.07 (d, ³*J*(H,H) = 7.6 Hz, 1 H, N⁴H), 4.88 (m, 2 H, N⁹H, N¹¹H), 4.57–4.50 (m, 1 H, C¹⁵H), 4.34–4.26 (m, 1 H, 1 C⁷H₂), 4.24–4.13 (m, 2 H, C⁵H, C¹²H), 4.05–3.93 (m, 2 H, C⁸H, 1 C⁷H₂), 1.74–1.25 (m, 21 H, 3 C¹H₃, 4 C²²H₂, 4 C²³H), 0.96–0.85 (m, 24 H, 8 C²³H₃). ¹³C NMR (CD₃OD): δ 175.9, 174.8, 173.7, 159.7, 158.1, 137.2, 129.6, 129.4, 129.3, 80.5, 68.4, 67.9, 53.5, 53.2, 52.1, 48.1, 42.9, 42.1, 41.6, 41.4, 28.7, 26.0, 25.8, 23.6, 23.39, 23.36, 23.3, 22.5, 21.93, 21.86. HR-ESI-MS: *m/z* 691.4612 (calcd 691.4646 for C₃₇H₆₂N₄O₈ + 1 H⁺).

Boc-(D)-leucine-ester-(L)-leucinol-urea-(D)-leucine-amide-(L)-leucine-Bn (10b). 9b (1.46 g, 3.00 mmol), 1a (0.69 g, 3.11 mmol), and DMAP (0.37 g, 3.00 mmol) were dissolved in CH₂Cl₂ (50 mL) and the mixture was cooled to 0 °C. To the cold solution was added EDC (0.86 g, 4.50 mmol). The solution was allowed to warm to room temperature and stirred for 60 h. The reaction mixture was quenched by the addition of silica gel. After the mixture was stirred for 4 h, the solvent was evaporated in vacuo. The solid residue was given on a column and purified via silica column chromatography (eluent: Et₂O). The crude product (2.20 g) was recrystallized from PE:CH₂Cl₂ to give 1.98 g (96%) of pure 10b. *R_f* 0.10 (PE:EA = 4:1). HPLC (2 × 150 mm Luna Phenyl-Hexyl 3 μm, acetonitrile:water, grad: 5 → 95 vol %

AN): $t_R = 23.55$ min (>99.0% peak area). ^1H NMR (400 MHz, CD_2Cl_2 , 20 °C): δ 7.39–7.29 (m, 5 H, C^{19-21}H), 7.15 (d, $^3J(\text{H},\text{H}) = 7.8$ Hz, 1 H, N^{14}H), 5.12 (dd, $J(\text{H},\text{H}) = 12.2$ Hz, $J(\text{H},\text{H}) = 19.5$ Hz, 2 H, C^{17}H_2), 5.05 (d, $^3J(\text{H},\text{H}) = 5.6$ Hz, 1 H, N^4H), 4.92 (d, $^3J(\text{H},\text{H}) = 7.3$ Hz, 1 H, N^9H), 4.82 (d, $^3J(\text{H},\text{H}) = 9.2$ Hz, 1 H, N^{11}H), 4.72–4.66 (m, 1 H, 1 C^7H_2), 4.62–4.55 (m, 1 H, C^{15}H), 4.20–4.09 (m, 2 H, C^5H , C^{12}H), 4.09–4.03 (m, 1 H, C^8H), 3.76 (d, $J(\text{H},\text{H}) = 9.6$ Hz, 1 H, 1 C^7H_2), 1.75–1.21 (m, 21 H, 3 C^1H_3 , 4 C^{22}H_2 , 4 C^{23}H), 0.97–0.83 (m, 24 H, 8 C^{23}H_3). ^{13}C NMR (CD_3OD): δ 175.9, 174.9, 173.7, 159.6, 158.2, 137.2, 129.6, 129.3, 129.2, 80.6, 67.9, 67.8, 53.73, 53.68, 52.2, 48.5, 42.9, 41.7, 41.3, 41.2, 28.8, 25.93, 25.87, 23.6, 23.35, 23.31, 22.3, 22.1, 21.9, 21.8. HR-ESI-MS: m/z 691.4651 (calcd 691.4646 for $\text{C}_{37}\text{H}_{62}\text{N}_4\text{O}_8 + 1 \text{H}^+$).

Acknowledgment. Generous support by the German Research Foundation (DFG via SFB 765) and the Fonds der Chemischen Industrie for providing a doctoral Kekulé-Fellowship to Sebastian Hartwig are gratefully acknowledged. Wacker Chemie AG, BASF AG, Bayer Industry Services, and Sasol Germany are thanked for generous donations of chemicals.

Supporting Information Available: Details of building block and oligomer synthesis as well as compound characterization data. This material is available free of charge via the Internet at <http://pubs.acs.org>.